



Cartilage injury and repair: assessment with magnetic resonance imaging

Tsou I Y Y, Yegappan M, Ong W S, Goh P O L, Tan J L, Chee T S G

ABSTRACT

Articular cartilage damage plays a major role in joint degeneration and dysfunction. Accurate assessment of the morphology and degree of cartilage wear is important in diagnosis, prognosis and management, particularly as many of these patients are young or participate in high-performance sports. Magnetic resonance imaging is able to directly evaluate such injuries, due to its high spatial resolution and excellent soft-tissue contrast resolution. This pictorial essay aims to demonstrate normal and damaged articular cartilage on MR imaging, as well as surgically-repaired cartilage.

Keywords: articular cartilage, cartilage damage, cartilage repair, magnetic resonance imaging

Singapore Med J 2006; 47(1):80-88

INTRODUCTION

All synovial joints in the body have hyaline cartilage lining the articular margins, which play a crucial role in proper joint function. Hyaline cartilage has two unique properties which serve this purpose: it is able to sustain loads of up to ten times body weight during daily activities such as walking, and is near-frictionless with an extremely low coefficient of friction^(1,2). It is continually synthesised and repaired to replace damage from mechanical wear, and is able to last for up to seven or eight decades.

Failure of normal cartilage function is a basic factor in the pathophysiology of osteoarthritis. Osteoarthritis is the most common form of arthritis, and its incidence and prevalence have been shown to increase by two to ten-fold from 30 to 65 years of age⁽³⁾. Radiography has traditionally been used in evaluation of osteoarthritis, however, actual cartilage loss is indirectly assessed by the reduction in joint space. In addition, technical differences in positioning make accurate reproducibility difficult, and this form of measurement has been shown

to be imprecise⁽⁴⁾. With its ability to perform multiplanar imaging and excellent soft tissue contrast resolution, coupled with advances in pulse sequence development, magnetic resonance (MR) imaging has been used to evaluate cartilage morphology and integrity^(5,6).

CARTILAGE STRUCTURE AND ANATOMY

Articular cartilage has a unique combination of porous, viscous and elastic properties which allow it to perform its functions. Although the term “hyaline” describes its amorphous appearance on light microscopy, it is actually highly fibrous. It is useful to conceptualise cartilage as a collagenous lattice, within which exist smaller water molecules and larger proteoglycan macromolecules. The collagen lattice has a differential structure within it, and can be divided into four zones or layers depending on the chondrocyte morphology and orientation, as well as the histological staining properties⁽¹⁾.

The deepest layer of cartilage is calcified, and serves to anchor the collagen lattice on to the underlying bone. This is separated from the next layer by a tide mark. The collagen fibrils within the next layer lie predominantly in a vertical (perpendicular to the cartilage surface) orientation, and this layer is known as the radial zone. The transitional zone above this has a more random orientation to the collagen fibrils, many of which lie in an oblique plane, to withstand shear forces. The most superficial layer consists of many collagen fibrils in a tangential (parallel to the cartilage surface) orientation, forming a thin layer of closely-packed horizontal leaves (Fig. 1).

The proteoglycan macromolecules within the lattice draws water into the cartilage substance by osmosis. In the normal physiological state, the stiff collagen lattice prevents maximal uptake of water⁽⁷⁾. This acts to distend the collagen lattice and keeps the fibrils under tension. This “inflated” state produces the compressive stiffness of cartilage and allows it to sustain loading. When there is disruption of the superficial layer from trauma or degeneration,

Department of
Diagnostic Radiology
Tan Tock Seng Hospital
11 Jalan Tan Tock Seng
Singapore 308433

Tsou I Y Y, MMed,
FRCR, FAMS
Consultant

Chee T S G, DMRD,
FRCR, FAMS
Senior Consultant
and Head

Department of
Orthopaedic Surgery
Tan Tock Seng
Hospital

Yegappan M, MBBS,
FRCSE, FRCSG
Consultant

Military Medicine
Institute
Singapore Armed
Forces
27 Medical Drive
DSO (Kent Ridge)
Building, #08-01
Singapore 117510

Ong W S, MBBS,
MSPMed, GCertSpNutr
Head

Sports Medicine and
Sports Science
Division
Singapore Sports
Council
National Stadium
15 Stadium Road
Singapore 397718

Goh P O L, MBBS, MS
Deputy Director

Island Sports Medicine
and Surgery
Gleneagles Medical
Centre
6 Napier Road, #09-05
Singapore 258499

Tan J L, FRCSE,
FRCSG, FAMS
Consultant Sports
Surgeon

Correspondence to:
Dr Ian Tsou Y Y
Tel: (65) 6357 8111
Fax: (65) 6357 8112
Email: ian_tsou@
tsh.com.sg

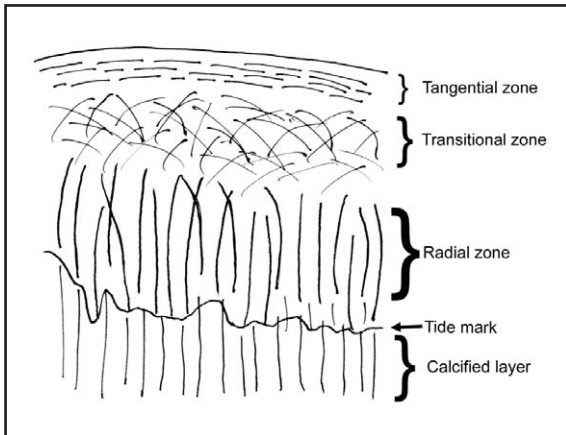


Fig. 1 Schematic diagram shows orientation of collagen fibrils within different layers of articular cartilage.

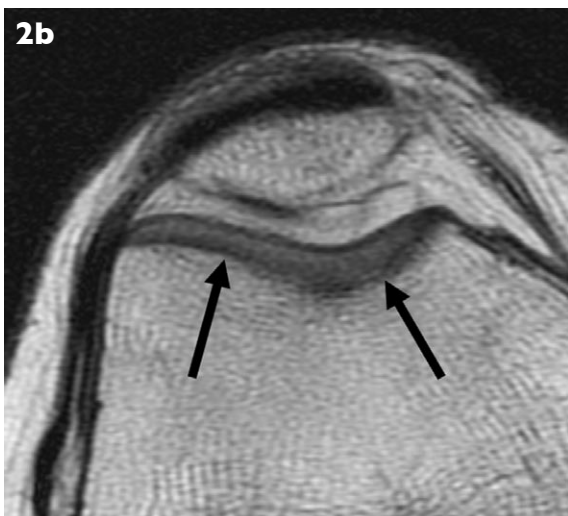


Fig. 2 Fast spin-echo proton-density MR images of normal-thickness articular cartilage over the (a) lateral femoral condyle (black arrows) and lateral tibial plateau (white arrow) in the sagittal plane, and (b) over the trochlear groove (black arrows) of the distal femur in the axial plane.

the surface fibrillation allows increased permeability of water, which is attracted into the cartilage from synovial fluid from the exposed negative charge of the macromolecules. This increase in the hydration of the cartilage, together with fragmentation of the macromolecules, renders the cartilage susceptible to mechanical stress and reduces its weight-bearing capacity. More load is then transferred to the subchondral bone, which responds by increasing bone deposition, and which then manifests as sclerosis.

NORMAL CARTILAGE APPEARANCE AND MR IMAGING SEQUENCES

The objective of MR imaging of cartilage is to evaluate surface integrity, cartilage thickness, matrix signal and subchondral margin and attachment to bone (Figs. 2a & b). The laminar appearance on histological specimens has been difficult to reproduce on clinical MR imaging, with best results *ex-vivo*, which were able to show a trilaminar appearance and accurate measurements of cartilage thickness^(8,9).

Grading of articular cartilage damage and ulceration is based on a modified Outerbridge classification system, where grade 0 is normal intact cartilage, grade 1 is chondral softening and blistering, grade 2 is a partial-thickness (less than 50%) defect or fissuring, grade 3 is a deeper (more than 50%) partial-thickness defect, and grade 4 is full-thickness cartilage loss with exposure of the subchondral bone⁽¹⁰⁾ (Figs. 3a-d). Early changes manifest as surface fibrillation, which at arthroscopy show a typical “crab-meat” appearance (Fig. 4). Focal areas of sharply-margined cartilage loss are likely to be due to shear or impaction injuries from recent trauma, whereas diffuse or larger areas of cartilage loss may be a result of chronic trauma or degeneration (Figs. 5-8). Cartilage delamination (Figs. 9a-c) and osteochondral lesions (Fig. 10) can also be evaluated with MR imaging.

Conventional T1-weighted and T2-weighted spin echo sequences are generally not able to evaluate cartilage signal and thickness well. T1-weighted images are relatively poor at demonstrating the cartilage-joint fluid interface, while on T2-weighted images, the deeper layers of cartilage merge with the subchondral bone, with the interface not being well discerned^(11,12) (Figs. 11a & b). Routine MR imaging without dedicated cartilage-specific sequences has a low (30% to 40%) sensitivity for cartilage defects in the knee⁽¹³⁾.

The International Cartilage Repair Society (ICRS) formed an articular cartilage imaging

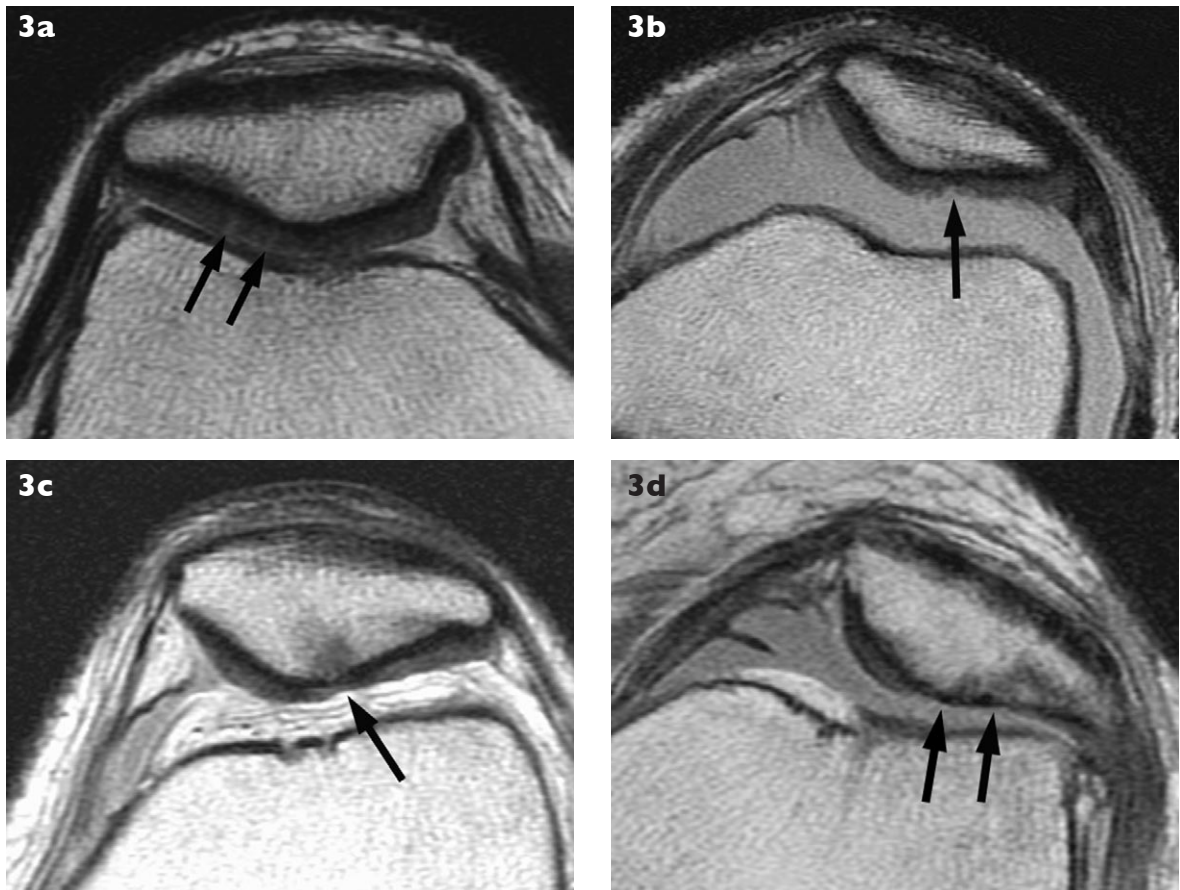


Fig. 3 Axial fast spin-echo proton-density MR images show varying degrees of articular cartilage wear at lateral facet of patella in different patients, illustrating the modified Outerbridge classification. Black arrows indicate site of cartilage abnormality.
 (a) Increased focal areas of signal intensity within normal-thickness cartilage indicative of matrix damage and increased fluid content.
 (b) Partial-thickness cartilage loss with surface fibrillation, affecting less than 50% of the cartilage thickness.
 (c) Greater degree of cartilage loss (more than 50% of thickness) but without exposure of subchondral bone. Underlying early sclerosis seen in subchondral bone immediately deep to the area of cartilage loss.
 (d) Complete cartilage loss with reactive sclerotic changes in the subchondral bone, indicating increased loading.



Fig. 4 Sagittal fast spin-echo proton-density MR image shows surface fibrillation on a focal area of the patellar articular cartilage (black arrow). The opposing trochlear cartilage is normal.

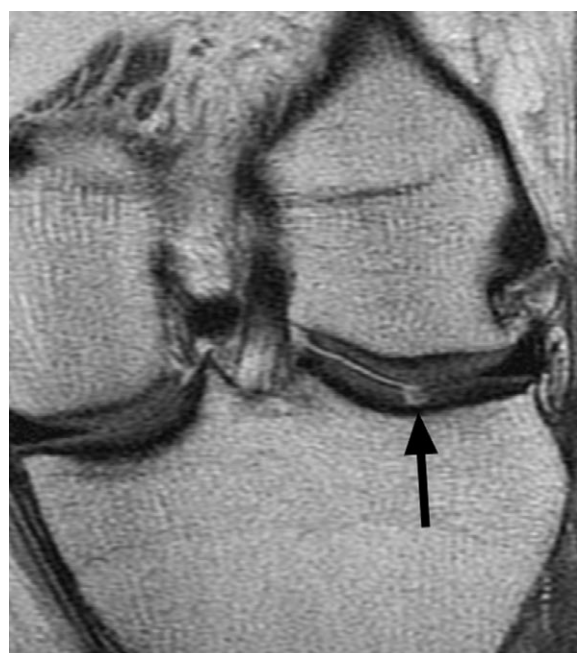


Fig. 5 Coronal fast spin-echo proton-density MR image shows a focal full-thickness defect in the articular cartilage over the lateral tibial plateau.



Fig. 6 Sagittal fast spin-echo proton-density MR image shows extensive delamination of the trochlear articular cartilage (white arrow), with a free cartilage flap (black arrow).



Fig. 7 Sagittal fast spin-echo proton-density MR image shows partial-thickness cartilage loss on the posterior aspect of the lateral femoral condyle (long black arrow), and full-thickness loss in the posterior aspect of the lateral tibial plateau (short black arrow). The primary injury is an oblique tear through the posterior horn of the lateral meniscus (white arrow), resulting in increased loading on the cartilage surfaces.

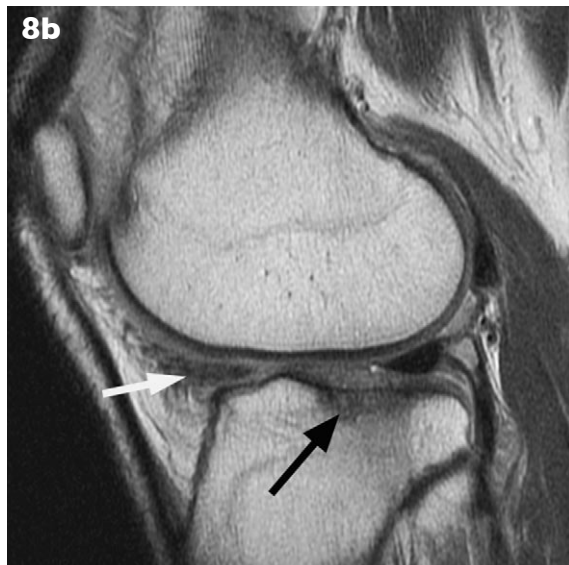
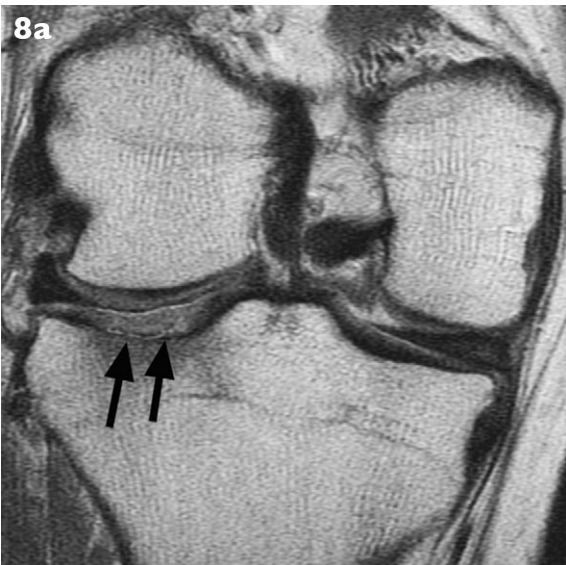


Fig. 8 (a) Coronal fast spin-echo proton-density MR image shows extensive fibrillation in articular cartilage over lateral tibial plateau, manifested as areas of ill-defined increased signal intensity (black arrows). The opposing femoral articular cartilage is normal. (b) Sagittal fast spin-echo proton-density MR image in the same patient shows prior tear in the anterior horn of the lateral meniscus (white arrow) and subchondral bone changes in the lateral tibial plateau (black arrow).

committee in 1998, with its main objective to develop an internationally-acceptable imaging protocol for optimal evaluation of cartilage. The committee released its recommendations in January 2000, with the two most widely available techniques being the fat-suppressed 3-dimensional spoiled gradient echo (3D-SPGR) sequence and proton-density weighted fast spin-echo (FSE) sequences⁽¹⁴⁾ (Figs. 12a & b).

Both techniques have been validated in patients at 1.0 and 1.5 Tesla field strengths. Published results for both techniques in the knee have been excellent, with sensitivities from 86-95%, specificities from 88-97%, accuracy from 83-92%, positive predictive values from 80-85% and negative predictive values from 91-97%, taking arthroscopy as the gold standard^(6,13,15).

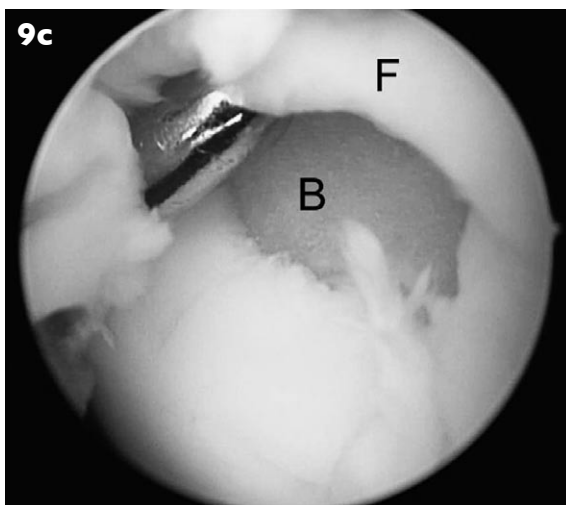


Fig. 9. (a) Sagittal and (b) coronal fast spin-echo proton-density MR images show fluid (black arrows) undermining a focal area of articular cartilage, indicating delamination. (c) Arthroscopy confirmed full-thickness delamination with exposure of subchondral bone surface (B) with elevation of the cartilage flap (F) by the probe.



Fig. 10 Coronal fast spin-echo proton-density MR image shows an osteochondral defect in the medial femoral condyle (black arrows), with abrupt termination of the overlying cartilage layer.

The two techniques have different advantages and disadvantages. The fat-suppressed 3D-SPGR sequence allows for thinner sections, down to 1mm thickness, which provides better definition of surface morphology. The fast spin-echo sequence utilises the magnetisation transfer effect, which makes it more sensitive for demonstration of signal abnormalities within the cartilage substance, before morphological defects appear. Other advantages of the fast spin-echo sequence are better visualisation of other soft tissue structures such as menisci and ligaments, and it is also less prone to susceptibility artifacts, which may be an issue in the post-surgical joint. Newer MR imaging sequences such as steady-state free precession and driven equilibrium fourier transform techniques have been reported to be able to achieve higher signal-to-noise (SNR) ratios, allowing good contrast between cartilage and adjacent tissue^(16,17) (Fig. 13).

The knee joint is particularly suited for cartilage evaluation, as the patella has the thickest articular cartilage in the body, and validation of imaging techniques is correlated with knee arthroscopy, which is widely used. However, other joints, such as the shoulder, wrist, hip and ankle can also be evaluated with similar MR techniques⁽¹⁸⁾ (Fig. 14).

CARTILAGE REPAIR IMAGING

The impetus in development of cartilage-specific MR imaging sequences is largely due to the feasibility of surgical techniques for cartilage repair, which have become well-established in sports medicine and orthopaedic surgery. The three broad categories are local stimulation of cartilage growth (which

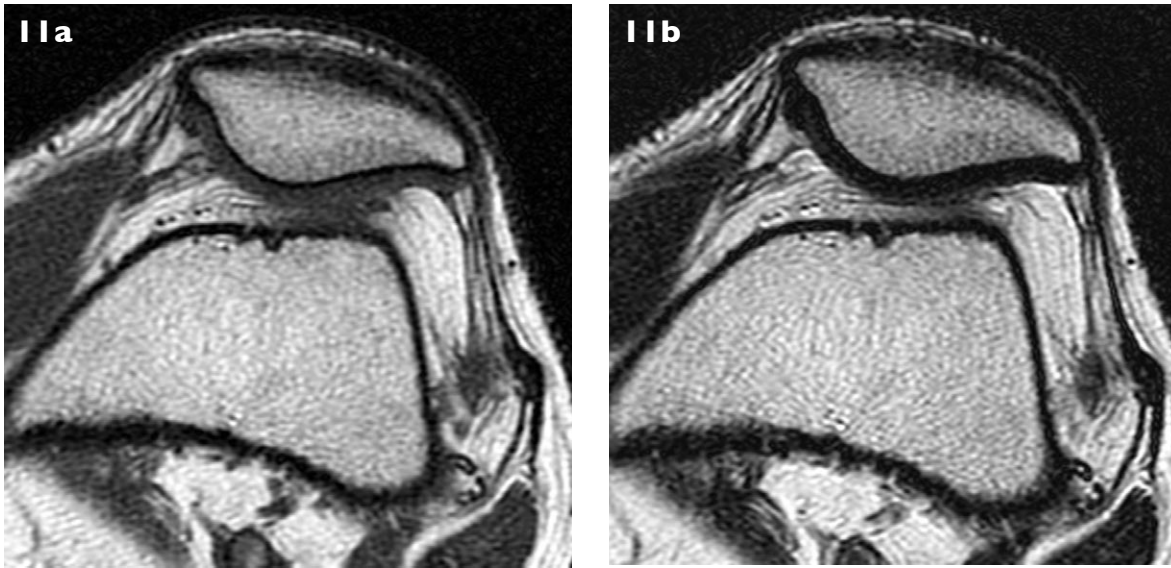


Fig. 11 Axial (a) T1-W and (b) T2-W MR images of the patella in the same patient show suboptimal distinction of articular cartilage from subchondral bone layer.



Fig. 12 Sagittal MR images show normal articular cartilage over the patella and trochlea on (a) fast spin-echo proton-density image (grey layer) and on (b) fat-suppressed spoiled gradient echo image (white layer).

include microfracture, drilling or abrasion), autologous transplantation of cartilage with either osteochondral elements or chondrocyte implantation, and allograft osteochondral transplantation⁽¹⁹⁾. In addition, significant ligament or meniscal tears in the knee should also be addressed, otherwise the transplanted or regenerated cartilage will still be subject to the same forces which caused the breakdown in the first place.

The marrow stimulation techniques aim to release stem cells from the subchondral bone at the

site of cartilage defect, which will differentiate into repair cartilage with time. With the microfracture technique, the repair cartilage is expected to be mostly fibrocartilage, rather than hyaline cartilage, and will be of different signal intensity⁽²⁰⁾ (Fig. 15). In autologous chondrocyte implantation, cultured chondrocytes are secured within the cartilage defect with an overlying periosteal patch⁽²¹⁾. This repair cartilage has been shown to change in signal intensity with time, possibly reflecting a change in composition, which is usually a combination of

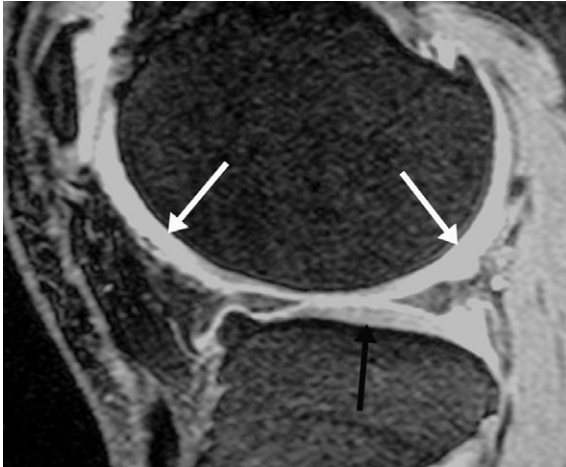


Fig. 13 Sagittal MR image obtained with the dual-excitation steady-state (DESS) sequence shows normal articular cartilage over the lateral femoral condyle (white arrows) and lateral tibial plateau (black arrow).

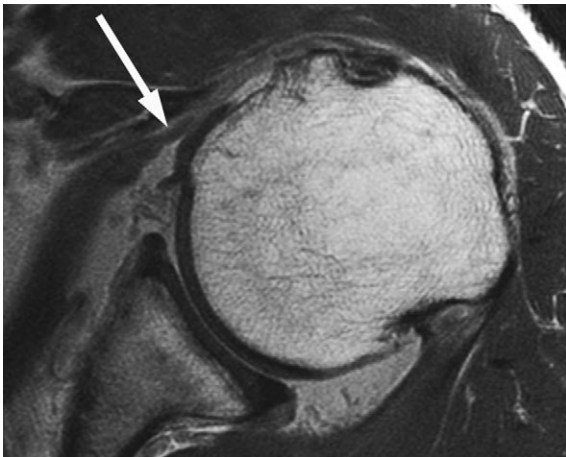


Fig. 14 Axial fast spin-echo proton-density MR image of the left shoulder shows normal articular cartilage over both the humeral head and glenoid process articular surfaces. The patient also has a tear in the subscapularis tendon (white arrow) with medial subluxation of the long head of the biceps tendon.

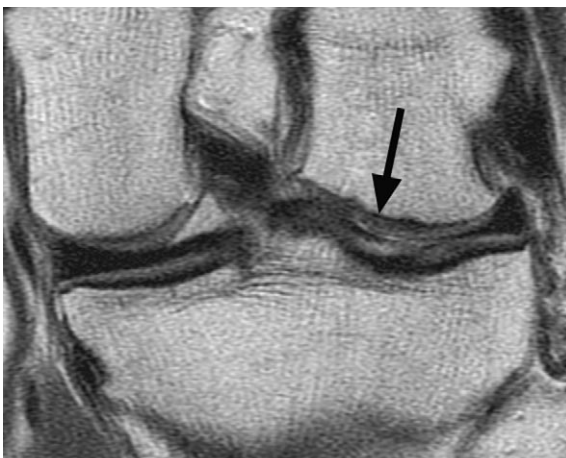


Fig. 15 Coronal fast spin-echo proton-density MR image shows repaired cartilage over the medial aspect of the lateral femoral condyle (black arrow), 4 years after a microfracture procedure was performed. The repair cartilage is of lower signal intensity and has some surface irregularity compared to the native articular cartilage. However, there is good fill of the defect with no subchondral bony changes.



Fig. 16 Sagittal fast spin-echo proton-density MR images (a) before and (b) 1 year after autologous chondrocyte implantation for a cartilage defect in the trochlea (black arrows). There is complete fill of the defect by a hyaline-like repair cartilage, without delamination or underlying bony hypertrophy.

fibrocartilage and hyaline-like articular cartilage⁽²²⁾ (Fig. 16). In osteochondral transplants, either with allograft or autograft, the main issues are incorporation of the bone plug into the native bone, and creation of a flush articular surface between the repair and native cartilage.

FUTURE DIRECTIONS

The next step forward in cartilage imaging will go beyond just imaging of the cartilage morphology, and will be able to non-invasively assess cartilage biochemistry. Possible parameters to evaluate are water content or hydration, collagen orientation and macromolecule concentration. Collagen fibre orientation is related to T2 relaxation times in T2 mapping, and related to diffusivity and fractional anisotropy in diffusion tensor imaging^(23,24). Delayed gadolinium-enhanced MR imaging has been able to evaluate glycosaminoglycan concentration in cartilage⁽²⁵⁾.

CONCLUSION

Morphological assessment of articular cartilage should be part of the routine MR imaging evaluation of joints, and in particular the knee. From a diagnostic perspective, MR imaging assessment of cartilage can be useful in evaluating common, mild-but-niggling sport-related conditions such as anterior knee pain, where it could help differentiate a cartilaginous aetiology of pain from other causes. MR imaging is valuable for detection of early cartilage injury or wear, before secondary osteoarthritis sets in, as well as in assessment of suitability and postoperative follow-up of surgical cartilage repair.

REFERENCES

- Mow VC, Ratcliffe A, Poole AR. Cartilage and diarthrodial joints as paradigms for hierarchical materials and structures. *Biomaterials* 1992; 13:67-97.
- Charnley J. The lubrication of animal joints in relation to surgical reconstruction by arthroplasty. *Ann Rheum Dis* 1960; 19:10-9.
- Oliveria SA, Felson DT, Reed JI, et al. Incidence of symptomatic hand, hip and knee osteoarthritis among patients in a health maintenance organization. *Arthritis Rheum* 1995; 38:1134-41.
- Fife R, Brandt K, Braunstein E, et al. Relationship between cartilage damage and radiographic joint space narrowing in early osteoarthritis of the knee. *Arthritis Rheum* 1990; 22:S117
- Abadie E, Ethgen D, Avouac B, et al. Recommendations for the use of new methods to assess the efficacy of disease-modifying drugs in the treatment of osteoarthritis. *Osteoarthritis Cartilage* 2004; 12:263-8.
- Potter HG, Linklater JM, Allen AA, et al. Magnetic resonance imaging of articular cartilage in the knee. *J Bone Joint Surg* 1998; 80A:1276-84.
- Maroudas A, Bayliss MT, Venn MF. Further studies on the composition of human femoral head cartilage. *Ann Rheum Dis* 1980; 39:514-23.
- Cova M, Toffanin R, Frezza F, et al. Magnetic resonance imaging of articular cartilage: ex vivo study on normal cartilage correlated with magnetic resonance microscopy. *Eur Radiol* 1998; 8:1130-6.
- Cova M, Toffanin R, Szomolanyi P, et al. Short-TE projection reconstruction MR-microscopy in the evaluation of articular cartilage thickness. *Eur Radiol* 2000; 10:1222-6.
- Outerbridge RE. The etiology of chondromalacia patellae. *J Bone Joint Surg Br* 1961; 43:752-7.
- Hayes CW, Conway WF. Evaluation of articular cartilage: radiographic and cross-sectional imaging techniques. *Radiographics* 1992; 12:409-42.
- Recht MP, Kramer J, Marcelis S, et al. Abnormalities of articular cartilage in the knee: analysis of available MR techniques. *Radiology* 1993; 187:473-8.
- Disler DG, McCauley TR, Kelman CG, et al. Fat-suppressed three-dimensional spoiled gradient-echo MR imaging of hyaline cartilage defects in the knee: comparison with standard MR imaging and arthroscopy. *Am J Roentgenol* 1996; 167:127-32.
- Recht M, Bobic V, Burstein D, et al. Magnetic resonance imaging of articular cartilage. *Clin Orthop Relat Res* 2001; (391 Suppl):S379-96.
- Wang SF, Cheng HC, Chang CY. Fat-suppressed three-dimensional fast spoiled gradient-recalled echo imaging: a modified FS 3D SPGR technique for assessment of patellofemoral joint chondromalacia. *Clin Imaging* 1999; 23:177-80.
- Rhuem S, Zanetti M, Romero J, Hodler J. MRI of patellar articular cartilage; evaluation of an optimized gradient-echo sequence. *J Magn Reson Imaging* 1998; 8:1246-51.
- Gold GE, Fuller SE, Hargreaves BA, Stevens KJ, Beaulieu CF. Driven equilibrium magnetic resonance imaging of articular cartilage: initial clinical experience. *J Magn Reson Imaging* 2005; 21:476-81.
- Haims AH, Moore AE, Schweitzer ME, et al. MRI in the diagnosis of cartilage injury in the wrist. *Am J Roentgenol* 2004; 182:1267-70.
- Recht M, White LM, Winalski CS, et al. MR imaging of cartilage repair procedures. *Skeletal Radiol* 2003; 32:185-200.
- Minas T, Nehrer S. Current concepts in the treatment of articular cartilage defects. *Orthopedics* 1997; 20:525-38.
- Brittberg M, Lindahl A, Nilsson A, et al. Treatment of deep cartilage defects in the knee with autologous chondrocyte transplantation. *N Engl J Med* 1994; 331:889-95.
- Brown WE, Potter HG, Marx RG, et al. Magnetic resonance imaging appearance of cartilage repair in the knee. *Clin Orthop Relat Res* 2004; 422:214-23.
- Xia Y, Moody JB, Burton-Wurster N, Lust G. Quantitative in-situ correlation between microscopic MRI and polarized light microscopy studies of articular cartilage. *Osteoarthritis Cartilage* 2001; 9:393-406.
- Filidoro L, Dietrich O, Weber J, et al. High-resolution diffusion tensor imaging of human patellar cartilage: Feasibility and preliminary findings. *Magn Reson Med* 2005; 53:993-8.
- Bashir A, Gray ML, Hartke J, Burstein D. Nondestructive imaging of human cartilage glycosaminoglycan concentration by MRI. *Magn Reson Med* 1999; 41:857-65.

SINGAPORE MEDICAL COUNCIL CATEGORY 3B CME PROGRAMME

Multiple Choice Questions (Code SMJ 200601A)

	True	False
Question 1: With regard to articular cartilage assessment:		
(a) Radiographs provide an indirect measurement of cartilage thickness.	<input type="checkbox"/>	<input type="checkbox"/>
(b) There is good reproducibility of radiographs taken at different times to allow for assessment of change.	<input type="checkbox"/>	<input type="checkbox"/>
(c) Conventional T1-weighted magnetic resonance (MR) images are not able to demonstrate the surface (cartilage-joint fluid interface) of articular cartilage well.	<input type="checkbox"/>	<input type="checkbox"/>
(d) Conventional T2-weighted MR images are not able to demonstrate the deep (cartilage-subchondral bone interface) of articular cartilage well.	<input type="checkbox"/>	<input type="checkbox"/>
Question 2: Regarding the structure of articular cartilage:		
(a) It consists of both a collagenous lattice and proteoglycan molecules.	<input type="checkbox"/>	<input type="checkbox"/>
(b) The collagen fibres in the radial zone have a circular orientation.	<input type="checkbox"/>	<input type="checkbox"/>
(c) The collagen fibres in the superficial zone are oriented parallel to the cartilage surface.	<input type="checkbox"/>	<input type="checkbox"/>
(d) The proteoglycan molecules function to attract and retain water molecules within the collagen matrix.	<input type="checkbox"/>	<input type="checkbox"/>
Question 3: With regard to evaluation of the articular cartilage:		
(a) MR imaging can evaluate both cartilage morphology and integrity.	<input type="checkbox"/>	<input type="checkbox"/>
(b) The patella has the thickest articular cartilage in the body.	<input type="checkbox"/>	<input type="checkbox"/>
(c) There are usually 4 zones or layers within articular cartilage, discernable at microscopy.	<input type="checkbox"/>	<input type="checkbox"/>
(d) The modified Outerbridge classification for articular cartilage damage has 4 grades, from zero to 3.	<input type="checkbox"/>	<input type="checkbox"/>
Question 4: Regarding MR imaging of articular cartilage:		
(a) The 4-layered appearance on microscopy can be accurately reproduced on in-vivo MR imaging.	<input type="checkbox"/>	<input type="checkbox"/>
(b) An early sign of cartilage damage is surface fibrillation.	<input type="checkbox"/>	<input type="checkbox"/>
(c) Both fat-suppressed 3-dimensional spoiled gradient echo (3D-SPGR) sequence and proton-density weighted fast spin-echo (FSE) sequences have been validated for cartilage imaging.	<input type="checkbox"/>	<input type="checkbox"/>
(d) The proton-density weighted FSE sequence is more prone to susceptibility artefacts, which may be seen in the post-surgical state.	<input type="checkbox"/>	<input type="checkbox"/>
Question 5: Regarding cartilage repair techniques:		
(a) These techniques include local stimulation, autologous cartilage transplantation and osteochondral transplantation.	<input type="checkbox"/>	<input type="checkbox"/>
(b) Microfracture is based on the differentiation of stem cells to form repair cartilage.	<input type="checkbox"/>	<input type="checkbox"/>
(c) Microfracture is usually expected to produce hyaline repair cartilage.	<input type="checkbox"/>	<input type="checkbox"/>
(d) Osteochondral transplants can be performed using either autografts or allografts.	<input type="checkbox"/>	<input type="checkbox"/>

Doctor's particulars:

Name in full: _____

MCR number: _____ Specialty: _____

Email address: _____

Submission instructions:**A. Using this answer form**

1. Photocopy this answer form.
2. Indicate your responses by marking the "True" or "False" box
3. Fill in your professional particulars.
4. Post the answer form to the SMJ at 2 College Road, Singapore 169850.

B. Electronic submission

1. Log on at the SMJ website: URL <<http://www.sma.org.sg/cme/smj>> and select the appropriate set of questions.
2. Select your answers and provide your name, email address and MCR number. Click on "Submit answers" to submit.

Deadline for submission: (January 2006 SMJ 3B CME programme): 12 noon, 25 February 2006**Results:**

1. Answers will be published in the SMJ March 2006 issue.
2. The MCR numbers of successful candidates will be posted online at <http://www.sma.org.sg/cme/smj> by 20 March 2006.
3. All online submissions will receive an automatic email acknowledgment.
4. Passing mark is 60%. No mark will be deducted for incorrect answers.
5. The SMJ editorial office will submit the list of successful candidates to the Singapore Medical Council.